The 8th European Congress on Computational Methods in Applied Sciences and Engineering
ECCOMAS Congress 2022
5 – 9 June 2022, Oslo, Norway

SIMPLE MODELING FOR STIFFNESS EVALUATION OF BOLTED JOINTS USING INTERFACIAL ELEMENT

YOSHINAO KISHIMOTO[*] AND YUKIYOSHI KOBAYASHI[*]

[*] Department of Mechanical Engineering
Tokyo City University
1-28-1 Tamazutsumi, Setagaya-ku, 158-8557 Tokyo, Japan
e-mail: ykishimo@tcu.ac.jp, www.tcu.ac.jp

Key words: Finite Element Method, Multi-scale Approach, Interfacial Stiffness.

Abstract. This study has developed a novel finite element named interfacial element which simulates the contact between microscale asperities at contact surfaces of bolted joints. In this element, the contact is assumed to be the Hertzian contact of elastic asperities whose peak heights obey the Gaussian distribution. Based on this assumption, the stiffness of the interfacial element is derived from the compressive stress and the surface texture of the interfaces. On the other hand, it is necessary for large-scale simulations that target the entire vehicle body to reduce the number of nodes and elements in the finite element models. This study has further proposed simple modeling for stiffness evaluation of bolted joints using the interfacial element. Finite element simulations by simplified models in which heads, axes and holes of bolts were ignored were conducted and compared with detailed models and hammering tests. The results revealed that the mean value of the natural frequency of the simplified models had good agreement with that of the detailed models and the hammering tests though the calculation accuracy of the simplified models were lower than the detailed models. The bolt heads and the nuts could be ignored by increasing the density of the bolt axes to be equal to the total weight.

1 INTRODUCTION

Bolted joints are one of major joining methods of dissimilar materials required to construct multi-material structures [1–4]. Bolted joints have high joint strength because the external load is supported by bolt axes. However, the stiffness of bolted joints easily changes depending on the surface texture at the contact surface of jointed members and the clamping force of the bolt and nut. This is caused by the contact state between the microscale asperities at the contact surfaces which affects the transmission of the force between the members. In particular, the effect of the clamping force is remarkable. The interfacial stiffness and the natural frequency of the jointed part decrease with the decrease of the clamping force. The previous study developed a novel finite element named interfacial element which simulates the contact between microscale asperities at contact surfaces of bolted joints [5,6]. In this element, the contact is assumed to be the Hertzian contact of elastic asperities whose peak heights obey the Gaussian distribution. Based on this assumption, the stiffness of the interfacial element is derived from the compressive stress and the surface texture of the interfaces. The surface texture parameters are the number of asperity peaks per unit area, mean radius of curvature at asperity

peaks and standard deviation of asperity peak heights those represent the randomness of the contour profile of the contact surface.

On the other hand, it is necessary for large-scale simulations that target the entire vehicle body to reduce the number of nodes and elements in the finite element (FE) models. Even when one hole is created in the FE model, the number of nodes and elements easily increases. This study has further proposed simple modeling for stiffness evaluation of bolted joints using the interfacial element. Finite element simulations by simplified models in which heads, axes and holes of bolts were ignored were conducted and compared with calculation results of detailed models and measurement results of hammering tests.

2 INTERFACIAL ELEMENT [5,6]

Figure 1 shows the contact model of nominally flat surfaces. As shown in the left of Fig. 1, the pieces 1 and 2 are joined by the compressive stress p_z. *z*-axis is defined along the normal direction of the interfaces of the pieces. *x*-axis and *y*-axis are defined to be normal to each other as shown in Fig. 1. The contact model describes the contacts of the spherical asperities shown in the middle of Fig. 1. The orthotropic model shown in the right of Fig. 1 simulates the interfacial stiffness. The total height of the asperities is L, and the gap between the mean planes of the asperity peak heights is d. The elastic modulus E_z, G_{yz} and G_{zx} are derived by the following process, and the elastic modulus on the other directions is set to zero.

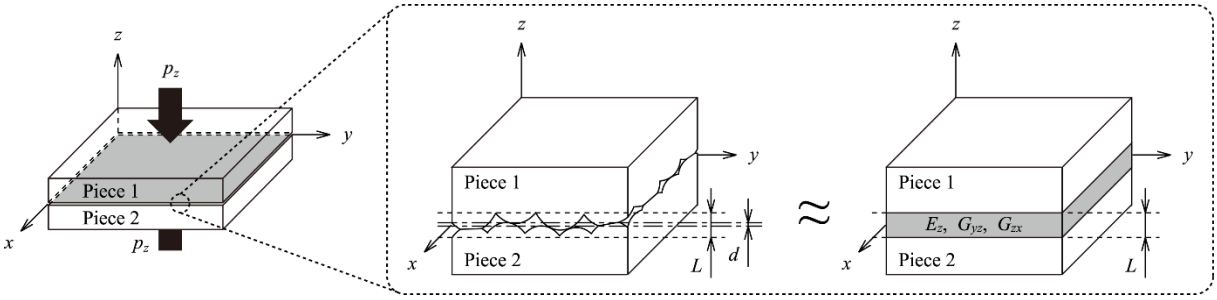

Figure 1: Contact model of nominally flat surfaces [6]

Assuming that the asperity peak heights obey the Gaussian distribution and the contact of asperities is the Hertzian contact [7,8], the relationship between the nominal compressive stress p_z and the gap d is described by using the homogenized elastic modulus C as follows [9].

$$p_z = C \cdot F_{5/2}(d) \tag{1}$$

where

$$F_m(d) = \frac{1}{\sqrt{2\pi}} \int_0^\infty \zeta^m \exp\left[-\frac{1}{2}\left(\zeta + \frac{d}{\sigma}\right)^2\right] d\zeta \tag{2}$$

$$\sigma = \sqrt{{\sigma_1}^2 + {\sigma_2}^2} \tag{3}$$

Using the subscript i as the identifier for the piece $i = 1, 2$, σ_i is the standard deviation of the asperity peak heights of the piece i. The homogenized elastic modulus C is described as follows.

$$C = \frac{64\pi\sigma^{\frac{5}{2}}\eta_1\eta_2}{15}\left(\frac{1}{\beta_1}+\frac{1}{\beta_2}\right)^{-\frac{3}{2}}\left(\frac{1-{\nu_1}^2}{E_1}+\frac{1-{\nu_2}^2}{E_2}\right)^{-1} \tag{4}$$

where η_i is the number of the asperity peaks per unit area, and β_i is the mean radius of the curvature at asperity peaks. E_i and ν_i are the Young's modulus and the Poisson's ratio of the base material of the piece i, respectively.

Assuming that the small displacement occurs in the vibration of the specimen, the *z*-direction Young's modulus of the interfaces can be described as follows.

$$E_z = -\frac{\partial p_z}{\partial(d/L)} = \left(\frac{F_{7/2}(d)}{F_{5/2}(d)}+\frac{d}{\sigma}\right)\frac{p_z \cdot L}{\sigma} \tag{5}$$

Similarly, Björklund derived the relationship between the shear stress and the displacement tangential to the interfaces under the compressive stress p_z based on the Mindlin's theory [10]. Assuming that the stiffness in the tangential direction to the interfaces is isotropic, the shear modulus is described as follows.

$$G_{yz} = G_{zx} = 4\left(\frac{1-{\nu_1}^2}{E_1}+\frac{1-{\nu_2}^2}{E_2}\right)\left(\frac{2-\nu_1}{G_1}+\frac{2-\nu_2}{G_2}\right)^{-1} E_z \tag{6}$$

where G_{yz} is the shear modulus at the *y*-surface in the *z*-direction, and G_{zx} is the shear modulus at the *x*-surface in the *z*-direction. G_i $(i = 1, 2)$ is the shear modulus of the base material of the piece i. In the finite element method (FEM) using the above model, the finite element whose elastic modulus are given by Eq. (5) and Eq. (6) is inserted into the interfaces. The finite element has been named as the interfacial element in this study.

3 INFLUENCE OF THREAD AND SEATING SURFACES

3.1 FE model

Before the investigation of the simple modeling, the influence of thread and seating surfaces of bolt and nut were investigated by the FEM of single bolted joint. Figure 2 shows the FE model of the single bolted joint (9190 nodes and 6687 elements). The constituent material of the bolted joint was set to steel (Young's modulus E_i = 200 GPa, Poisson's ratio ν_i = 0.3, Density = 7800 kg/m^3). The surface texture parameters were set to reference values as shown in Table 1. The interfacial element was applied on the thread and the seating surfaces. The fixing element is connected to the main body in order to stably compute the rigid body mode. The length of the bolt axis was given as three patterns (L = 20, 50, 105 mm).

Table 1: Surface texture parameters of bolt, nut and cylindrical collar

		Number of asperity peaks per unit area η_i [/mm^2]	Mean radius of curvature at asperity peaks β_i [μm]	Standard deviation of asperity peak heights σ_i [μm]
Bolt		24221	9.750	0.413
Nut		13348	5.604	2.862
Cylindrical collar	vs. Bolt	4841	5.977	1.468
	vs. Nut	8180	7.303	0.636

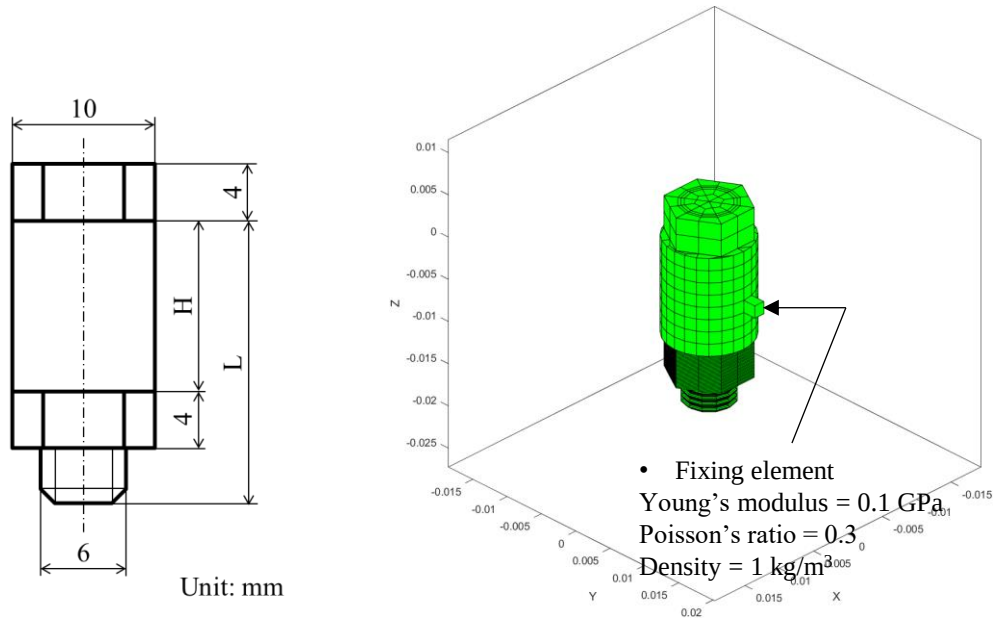

Figure 2: Schematic and finite element model of single bolted joint

3.2 Results and discussion

Figures 3 and 4 show the calculation results of the natural frequency of the single bolted joint. The natural frequency of the rigid body modes is constant subjected to the clamping force because the interfacial elements have no deformation in these rigid body modes as shown in

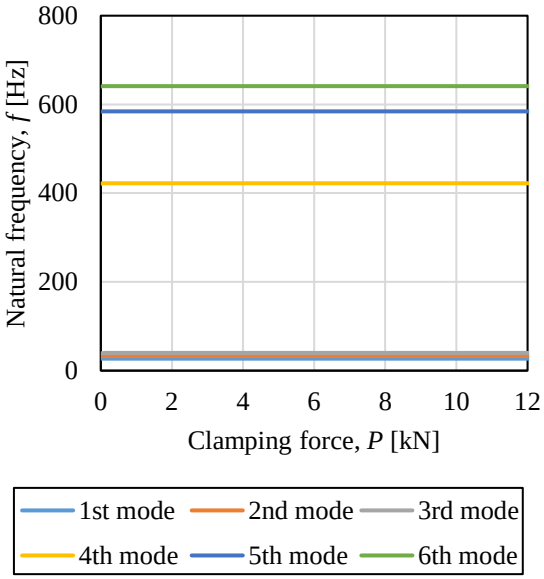

Figure 3: Natural frequency of rigid body modes (L = 20 mm)

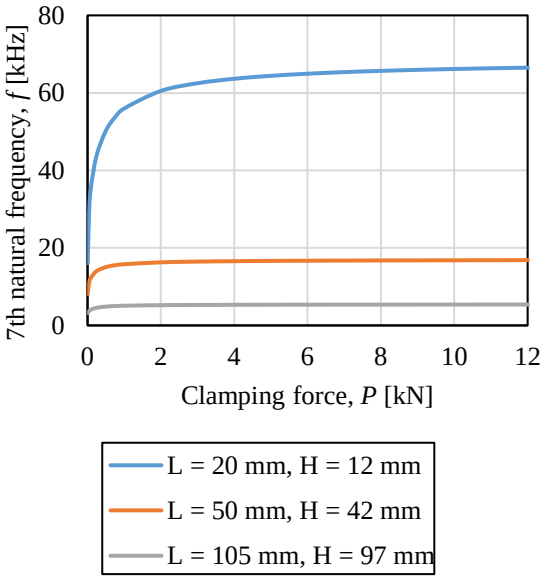

Figure 4: Natural frequency of 7th mode with different length of bolt axis

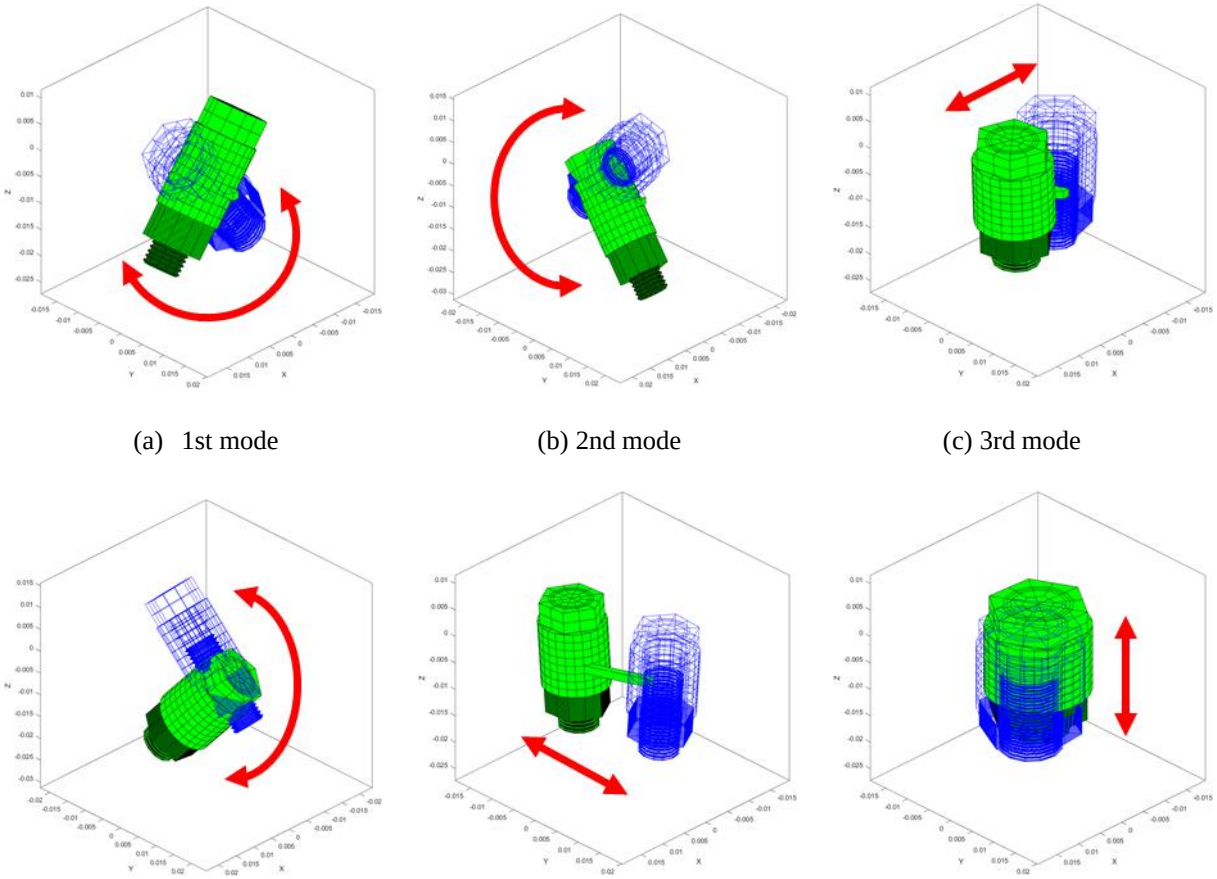

(a) 1st mode (b) 2nd mode (c) 3rd mode

(d) 4th mode (e) 5th mode (f) 6th mode

Figure 5: Vibration shapes of single bolted joint (L = 20 mm)

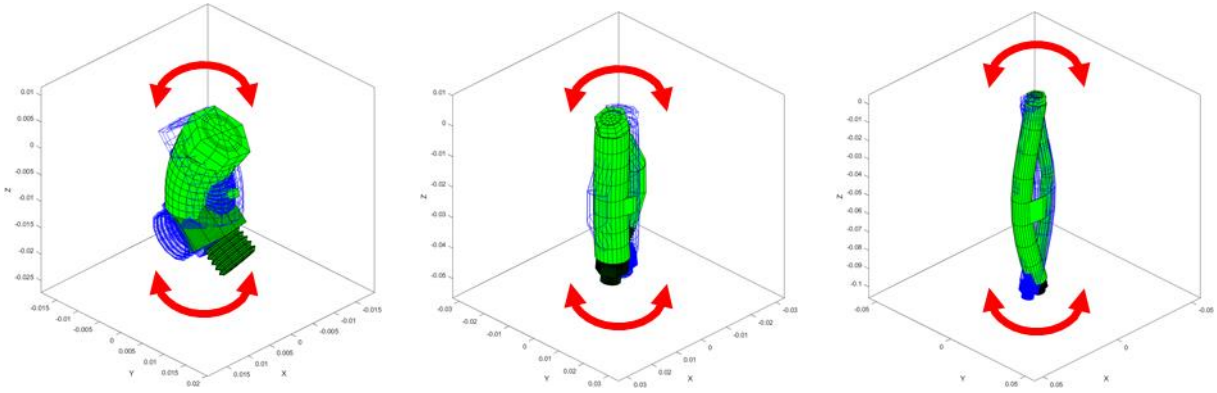

(a) 7th mode, L = 20 mm (b) 7th mode, L = 50 mm (c) 7th mode, L = 105 mm

Figure 6: 7th vibration shape of single bolted joint with different length of bolt axis

Fig. 5. The natural frequency of the 7th mode which is the lowest mode except the rigid body modes is affected by the interfacial stiffness of the thread and the seating surfaces and increases with the increase of the clamping force. The vibration shape is the 1st bending deformation as shown in Fig. 6. Moreover, the natural frequency increases with the decrease of bolt axis. The natural frequency will be higher than 20 ~ 70 kHz when the bolt axis is shorter than 20 mm. The influence of the thread and seating surfaces will be small on the natural frequency under 20 kHz and the bolt axis under 20 mm.

4 INFLUENCE OF BOLT HEADS, AXES AND HOLES

4.1 FE model and hammering test

The thick plates joint and the thin plates joint were prepared as shown in Figs 7 and 8. These joints consist of steel (Young's modulus E_i = 200 GPa, Poisson's ratio ν_i = 0.3, Density = 7800 kg/m^3). In the hammering tests, the natural frequency was obtained from the time history of

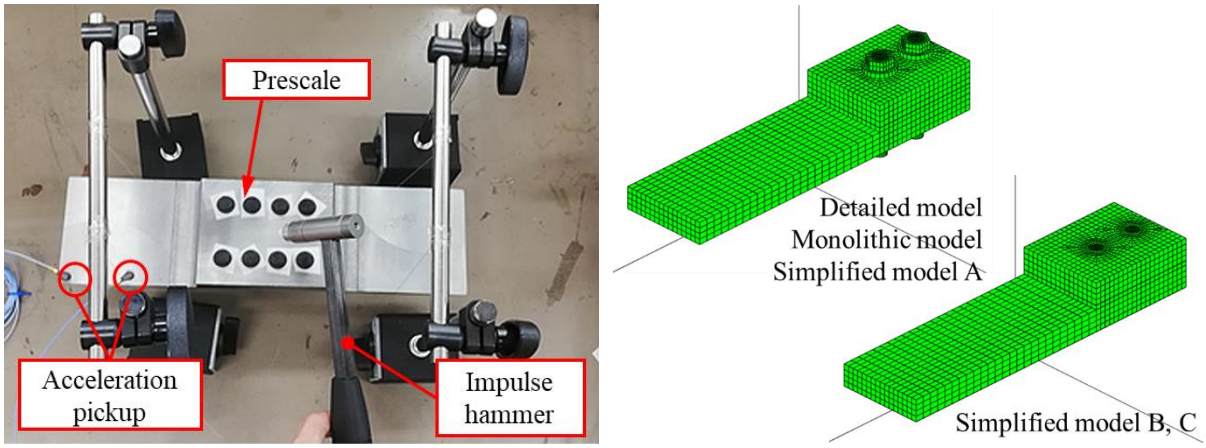

Figure 7: Thick plates joint and its finite element models

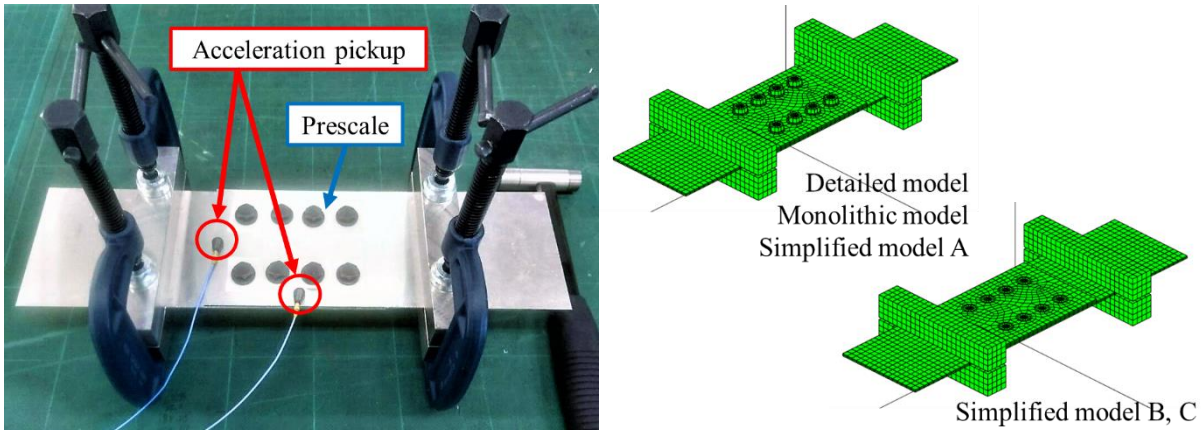

Figure 8: Thin plates joint and its finite element models

the acceleration just after the impact by the impulse hammer. The clamping force was measured by inserting the pressure measurement films (Prescale made by Fujifilm Corporation) into the seating surfaces of the bolts. The monolithic specimen whose shape is same as the thick plates joint was also tested. The monolithic specimen is the T-shaped thick plate clamped by 8 sets of bolt and nut.

The number of nodes and elements of each model is shown in Table 2. The interfacial element was applied only on the interfaces of the plates. The surface texture parameters were

Table 2: Number of nodes and elements in each model

	Thick plates joint		Thin plates joint	
	Nodes	Elements	Nodes	Elements
Detailed model Monolithic model	13002	10521	12138	8702
Simplified model A	12186	10329	11662	8894
Simplified model B, C	10104	8482	9214	6782

Table 3: Surface texture parameters of plates

	Number of asperity peaks per unit area η_i [/mm^2]	Mean radius of curvature at asperity peaks β_i [μm]	Standard deviation of asperity peak heights σ_i [μm]
Short thick plate	11346	3.247	2.189
Long thick plate	9311	6.012	2.493
Thin plate	25328	27.75	0.151

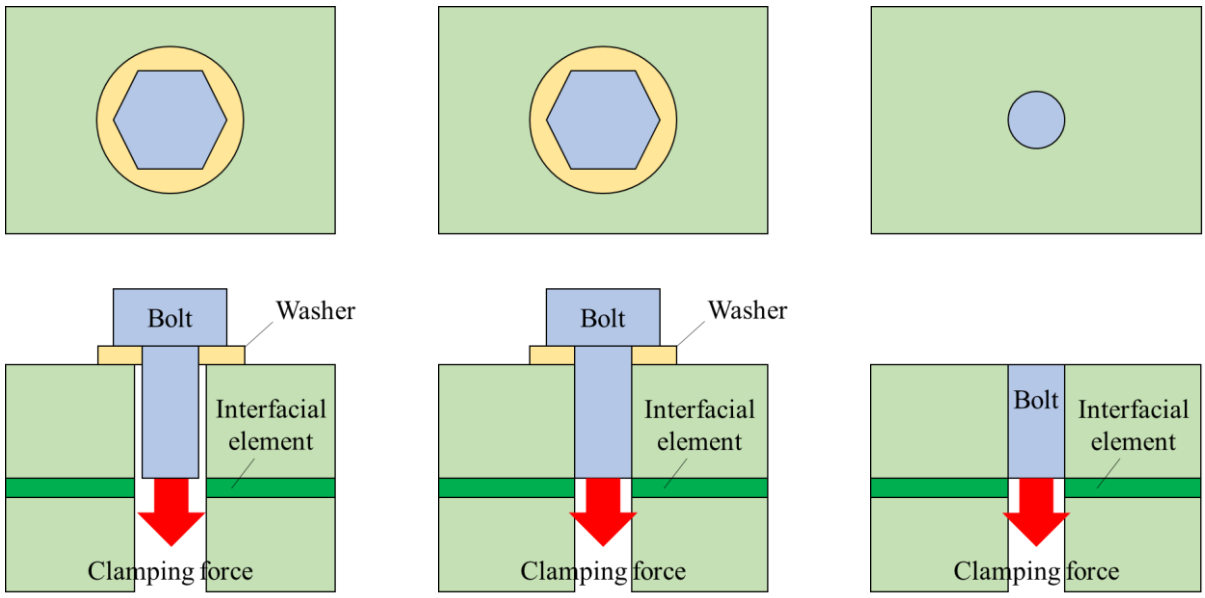

(a) Detailed model and monolithic model (b) Simplified model A (c) Simplified model B and C

Figure 9: Simplification of bolt heads, axes and holes

measurement values as shown in Table 3. The FE model of the thick plates joint is the 1/4 model. The monolithic models in which the material constants of the interfacial element were set to those of steel was also prepared in order to investigate the influence of the interfacial stiffness between the plates. Figure 9 shows the schematic of the simplification of the bolt heads, axes and holes. Taking account of the results of the chapter 3, the contacts of the thread and the seating surfaces were ignored. The bolt axes were formed as solid shafts. The simplified model A ignored the bolt holes. The interfaces between the bolt axes and the plates were formed by common nodes. The clampimg force would be transmitted to the interfacial elements as compressive force through the interfaces between the bolt axis and the plate as shearing force. The simplified model B and C ignored the bolt heads and the nuts. The transimisstion process of the clamping force is same as the simplified model A. Because the total weight of the bolted joints would reduce by the amount of the bolt heads and the nuts in the simplified model B, the density of the bolt axes in the simplified model C were increased to be equal to the simplified model A (Density = 18000 kg/m^3 in the thick plates joint, 62000 kg/m^3 in the thin plates joint).

4.2 Results and discussion

Figures 10 and 11 show the natural frequency of the thick plates joint and the thin plates joint, respectively. The natural frequency is the 1st bending mode which is the lowest natural

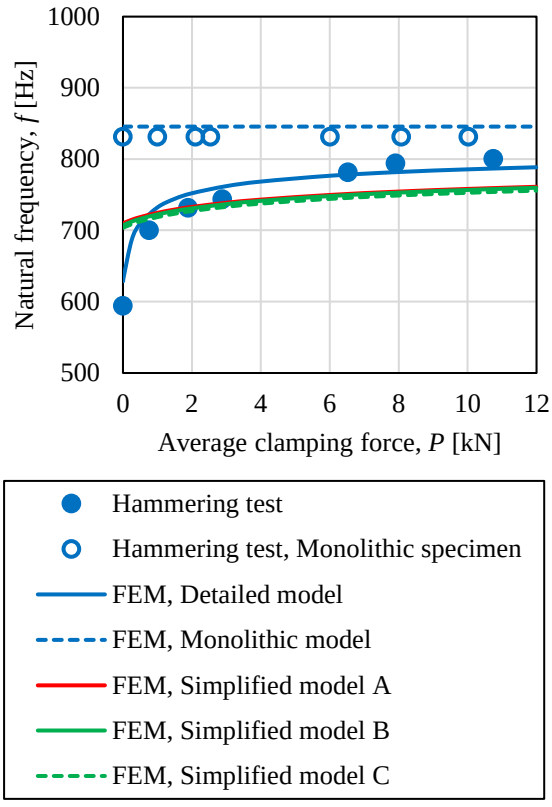

Figure 10: Natural frequency of thick plates joint

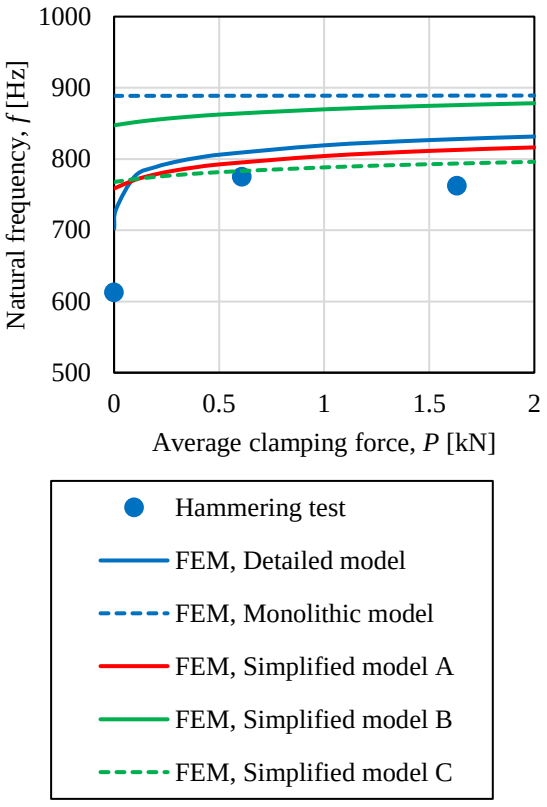

Figure 11: Natural frequency of thin plates joint

frequency except the rigid body modes as shown in Figs 12 and 13. In the hammering tests, the natural frequency of the thick plates joint and the thin plates joint increases with the increase of the clamping force. On the other hand, the natural frequency of the monolithic specimen is constant even if the clamping force is increased. Therefore, the natural frequency is affected by the interface between the plates, and the influence of the thread and the seating surfaces is small because the natural frequency of the monolithic specimen is constant.

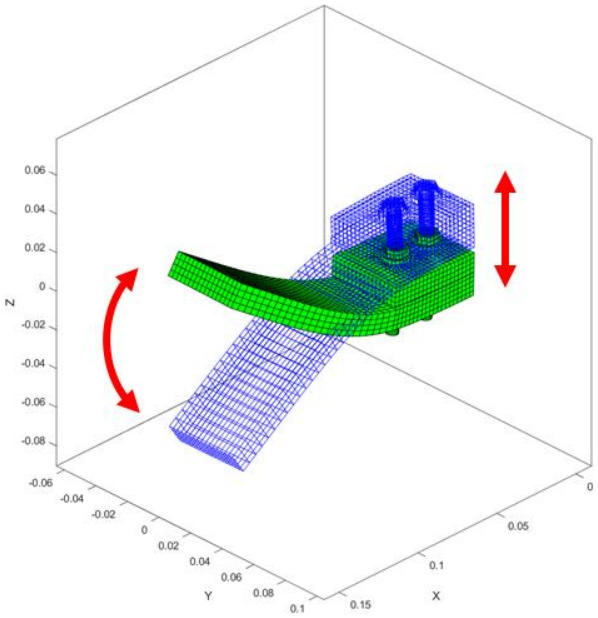

Figure 12: Vibration shape of thick plates joint

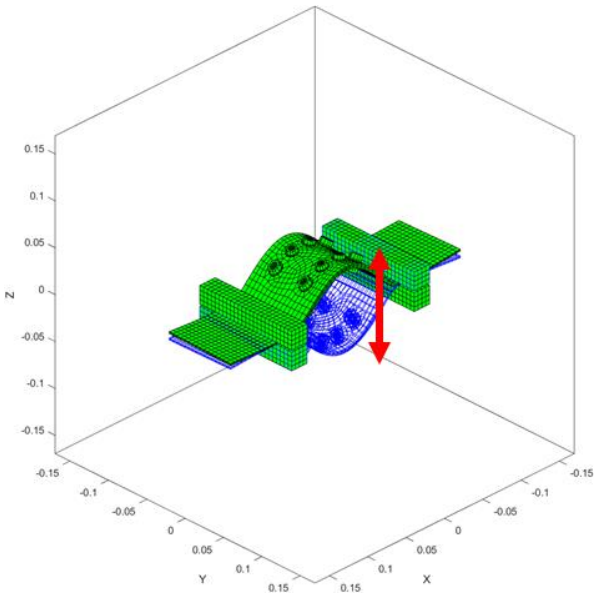

Figure 13: Vibration shape of thin plates joint

In Fig. 10, the calculation result of the detailed model agrees with the hammering test. Hence, the interfacial element successfully simulates the relationship between the natural frequency and the clamping force. The simplified models agree with each other. It seems that the influence of the bolt heads and the nuts is small because the bolt heads and the nuts are relatively smaller than the plates. The mean values of the natural frequency of the simplified models have good agreement with the detailed model and the hammering test. The reduction of the calculation accuracy depends on the presence or absence of the bolt holes.

In Fig. 11, the natural frequency of the detailed model is closer to the hammering test than the monolithic model. The simplified models A and C agree with the mean value of the detailed model. The simplified model B is higher than the hammering test, the detailed model and the simplified models A, C. It is difficult to just ignore the influence of the bolt heads and the nuts in the thin plates joint. In this situation, the bolt head and the nut could be ignored by increasing the density of the bolt axes to be equal to the total weight in the simplified model.

5 CONCLUSIONS

This study has proposed simple modeling for stiffness evaluation of bolted joints using the interfacial element based on the investigation of the influence of thread surfaces, seating

surfaces, bolt heads, bolt axes and holes. From the results of the numerical calculations and the hammering tests, the natural frequency of the detailed models and the simplified models was closer to the values of the hammering tests though the calculation accuracy of the simplified models were lower than the detailed models. The bolt heads and the nuts could be ignored by increasing the density of the bolt axes to be equal to the total weight in the simplified models. This work was supported by JSPS KAKENHI Grant Number JP18K03849 and JP21K03776.

REFERENCES

[1] Catalanotti, G., Camanho, P. P., Ghys, P. and Marques, A. T. An efficient design method for multi-material bolted joints used in the railway industry. *Composite Structures* (2011) **94 (1)**:246-252.

[2] Coelho, A. M. G. and Mottram, J. T. A review of the behaviour and analysis of bolted connections and joints in pultruded fibre reinforced polymers. *Materials & Design* (2015) **74**:86-107.

[3] Hammami, C., Balmes, E. and Guskov, M. Numerical design and test on an assembled structure of a bolted joint with viscoelastic damping. *Mechanical Systems and Signal Processing* (2016) **70-71**:714-724.

[4] Nichols, J. M., Trickey, S. T., Seaver, M., Motley, S. R. and Eisner, E. D. Using ambient vibrations to detect loosening of a composite-to-metal bolted joint in the presence of strong temperature fluctuations. *Transactions of the ASME, Journal of Vibration and Acoustics* (2006) **129 (6)**:710-717.

[5] Kishimoto, Y., Kobayashi, Y., Ohtsuka, T., Matsumoto, A. and Niizuma, M., Estimation method of interfacial stiffness of bolted joint in multi-material structure by inverse analysis, *Mechanical Engineering Journal* (2019) **6 (3)**:DOI: 10.1299/mej.18-00471.

[6] Kishimoto, Y. Kobayashi, Y. Ohtsuka, T. Shinohara, T. and Jimbo, N. Interfacial element for finite element modal analysis of bolted joints. *Proceedings of the 14th WCCM-ECCOMAS Congress 2020* (2021) DOI: 10.23967/wccm-eccomas.2020.180.

[7] Mindlin, R. D. Compliance of elastic bodies in contact. *Transactions of the ASME, Journal of Applied Mechanics* (1949) **16 (3)**:259-268.

[8] Mindlin, R. D., Mason, W. P., Osmer, J. F. and Deresiewicz, H. Effects of an oscillating tangential force on the contact surfaces of elastic spheres. *Proceedings of the 1st U.S. National Congress of Applied Mechanics, ASME* (1952) **1**:203-208.

[9] Greenwood J. A. and Tripp, J. H. The contact of two nominally flat rough surfaces. *Proceedings of the Institution of Mechanical Engineers* (1970) **185**:625-633.

[10] Björklund, S. A random model for micro-slip between nominally flat surfaces. *Transactions of the ASME, Journal of Tribology* (1997) **119**:726-732.